The Plant Cell, Vol. 25: 728–743, February 2013, www.plantcell.org

The *SUD1* Gene Encodes a Putative E3 Ubiquitin Ligase and Is a Positive Regulator of 3-Hydroxy-3-Methylglutaryl Coenzyme A Reductase Activity in *Arabidopsis*[C][W]

Verónica G. Doblas,[a,1] Vítor Amorim-Silva,[b,1] David Posé,[a] Abel Rosado,[a] Alicia Esteban,[a] Montserrat Arró,[c,d] Herlander Azevedo,[b] Aureliano Bombarely,[a] Omar Borsani,[e] Victoriano Valpuesta,[a] Albert Ferrer,[c,d] Rui M. Tavares,[b] and Miguel A. Botella[a,2]

[a] Instituto de Hortofruticultura Subtropical y Mediterránea, Universidad de Málaga–Consejo Superior de Investigaciones Científicas, Departamento de Biología Molecular y Bioquímica, Facultad de Ciencias, Universidad de Málaga, 29071 Malaga, Spain
[b] Center for Biodiversity, Functional and Integrative Genomics, Plant Functional Biology Center, University of Minho, Campus de Gualtar, 4710-057 Braga, Portugal
[c] Department of Molecular Genetics, Centre for Research in Agricultural Genomics (Consejo Superior de Investigaciones Científicas-Institut de Recerca i Tecnologia Agroalimentàries-Universidad Autónoma de Barcelona-Universidad de Barcelona), Bellaterra-Cerdanyola del Vallés, 08193 Barcelona, Spain
[d] Department of Biochemistry and Molecular Biology, Faculty of Pharmacy, University of Barcelona, 08028 Barcelona, Spain
[e] Laboratorio de Bioquímica, Departamento de Biología Vegetal, Facultad de Agronomía, Universidad de la República, Montevideo CP12900, Uruguay

The 3-hydroxy-3-methylglutaryl-CoA reductase (HMGR) enzyme catalyzes the major rate-limiting step of the mevalonic acid (MVA) pathway from which sterols and other isoprenoids are synthesized. In contrast with our extensive knowledge of the regulation of HMGR in yeast and animals, little is known about this process in plants. To identify regulatory components of the MVA pathway in plants, we performed a genetic screen for second-site suppressor mutations of the *Arabidopsis thaliana* highly drought-sensitive *drought hypersensitive2* (*dry2*) mutant that shows decreased squalene epoxidase activity. We show that mutations in *SUPPRESSOR OF DRY2 DEFECTS1* (*SUD1*) gene recover most developmental defects in *dry2* through changes in HMGR activity. *SUD1* encodes a putative E3 ubiquitin ligase that shows sequence and structural similarity to yeast Degradation of α factor (Doα10) and human TEB4, components of the endoplasmic reticulum–associated degradation C (ERAD-C) pathway. While in yeast and animals, the alternative ERAD-L/ERAD-M pathway regulates HMGR activity by controlling protein stability, SUD1 regulates HMGR activity without apparent changes in protein content. These results highlight similarities, as well as important mechanistic differences, among the components involved in HMGR regulation in plants, yeast, and animals.

INTRODUCTION

For sessile organisms such as plants, metabolic plasticity is essential to survive in their changing environments (Nicotra et al., 2010). A good example of this plasticity is the thousands of isoprenoid compounds and derivatives that higher plants synthesize from the five-carbon building units isopentenyl diphosphate (IPP) and its isomer dimethylallyl diphosphate (Bouvier et al., 2005). Plants synthesize IPP and dimethylallyl diphosphate by two independent pathways: the mevalonic acid (MVA) pathway, which produces cytosolic IPP (McGarvey and Croteau, 1995; Newman and Chappell, 1999); and the methylerythritol phosphate pathway, which is localized in the plastids (Eisenreich et al., 2001; Rodríguez-Concepción and Boronat, 2002). In higher plants, isoprenoids carry out numerous essential roles in developmental processes, including respiration, photosynthesis, growth, and reproduction, as well as adaptation to environmental challenges and involvement in plant defense mechanisms against different types of organisms (Tholl and Lee, 2011; Hemmerlin et al., 2012).

The main MVA-derived isoprenoid end products in plants are sterols, which are integral components of the membrane and are essential for plant growth and developmental processes. Other important MVA products are the steroid hormones brassinosteroids, dolichols, which are involved in protein glycosylation, and the prenyl groups used for protein prenylation and cytokinin biosynthesis (Benveniste, 2004; Phillips et al., 2006; Schaller, 2010). A number of studies over the years have shown the importance of correct sterol composition in plants because of their roles in embryonic pattern formation (Jang et al., 2000), cell division, elongation and polarity (Schrick et al., 2000; Willemsen et al., 2003; Men et al., 2008), vascular patterning (Carland et al.,

[1] These authors contributed equally to this work.
[2] Address correspondence to mabotella@uma.es.
The author responsible for distribution of materials integral to the findings presented in this article in accordance with the policy described in the Instructions for Authors (www.plantcell.org) is: Miguel A. Botella (mabotella@uma.es).
[C] Some figures in this article are displayed in color online but in black and white in the print edition.
[W] Online version contains Web-only data.
www.plantcell.org/cgi/doi/10.1105/tpc.112.108696

2010), cellulose accumulation (Schrick et al., 2004), reactive oxygen species (ROS) production (Posé et al., 2009), and normal microRNA function (Brodersen et al., 2012). Still, little is known about the mechanisms and downstream targets by which isoprenoids in general, and sterols in particular, influence these processes (Boutté and Grebe, 2009; Clouse, 2002).

The enzyme 3-hydroxy-3-methylglutaryl-CoA reductase (HMGR) is considered the major rate-limiting enzyme controlling the metabolic flux in the early steps of the MVA pathway (Hemmerlin et al., 2012). The genome of *Arabidopsis thaliana* contains two differentially expressed HMGR genes, *HMG1* and *HMG2* (Enjuto et al., 1994), encoding three HMGR isoforms: HMGR1S (short isoform), HMGR1L (long isoform), and HMGR2. HMGR1S and HMGR1L are both encoded by the *HMG1* gene and are identical in sequence, except for an N-terminal extension of 50 amino acid residues in HMGR1L (Lumbreras et al., 1995). HMGR1S has been proposed to have a housekeeping role, whereas HMGR1L and HMGR2 have a more specialized function, which might be required in particular cell types or at specific developmental stages (Suzuki et al., 2004, 2009). All plant HMGR variants are targeted to the endoplasmic reticulum (ER) and have the same topology in the membrane (Campos and Boronat, 1995). The diverged N-terminal region and the conserved catalytic domain are located in the cytosol, whereas only a short stretch of amino acids connecting the two transmembrane (TM) segments is in the ER lumen. Plant HMGR is modulated by a variety of developmental and environmental signals, and it has been proposed that major changes in HMGR activity are determined at the transcriptional level, whereas posttranscriptional regulation allows a finer and faster adjustment (Hemmerlin et al., 2012). In fact, evidence of posttranslational regulation of HMGR in *Arabidopsis* plants with enhanced or depleted flux through the sterol biosynthetic pathway has been obtained (Nieto et al., 2009). Similarly, inhibition of squalene epoxidase (SQE) activity in tobacco (*Nicotiana tabacum*) Bright Yellow-2 cells using terbinafine also triggers an increase in HMGR activity, even though it does not induce changes in the HMGR transcript levels (Wentzinger et al., 2002). Mechanistically, a protein phosphatase 2A (PP2A) has been recently identified as a negative regulator of *Arabidopsis* HMGR activity and protein levels (Leivar et al., 2011). Still, proteins involved in the posttranscriptional regulation of plant HMGR are mostly uncharacterized.

In plants, SQEs catalyze the conversion of squalene, the first committed precursor of essential MVA-derived isoprenoids, to 2,3-oxidosqualene (Rasbery et al., 2007; Posé et al., 2009; Schaller, 2010). The *Arabidopsis drought hypersensitive2* (*dry2/sqe1-5*) mutant was identified by its extreme hypersensitivity to drought stress, altered stomatal responses, and root defects. Chemical analysis indicated that the *dry2/sqe1-5* mutant has altered sterol composition in roots but wild-type sterol composition in shoots, indicating an essential role for SQE1 in root sterol biosynthesis. Importantly, the stomatal and root defects of the *dry2/sqe1-5* mutant are associated with altered production of ROS, establishing a previously unknown link between the MVA pathway and ROS (Posé et al., 2009).

The *dry2/sqe1-5* allele contains a point mutation in the 4th exon that produces a substitution of a conserved Gly by an Arg, resulting in reduced epoxidase activity (Posé et al., 2009). In contrast with the null alleles of *SQE1* that are sterile, *dry2/sqe1-5* plants are fertile, and this characteristic enables its use for genetic analyses. In this work, we used the hypomorphic *dry2/sqe1-5* mutant allele to perform a genetic screen for second-site suppressor mutations to identify new genetic components regulating the MVA pathway. Several mutants (named *sud* for *suppressors of dry2 defects*) that reversed most of the *dry2/sqe1-5* developmental phenotypes were isolated. As a result, we identified a regulatory element, *SUD1*, which encodes a protein with sequence and structural homology to the E3 ubiquitin ligases Degradation of α factor (Doa10) in yeast and TEB4 in humans (i.e., proteins that are involved in the endoplasmic reticulum–associated protein degradation [ERAD] pathway). Our results indicate that SUD1 functions as a positive posttranscriptional regulator of HMGR activity in *Arabidopsis*.

RESULTS

Phenotypic Characterization of the *dry2* Suppressors

To identify undescribed elements that regulate the isoprenoid biosynthetic pathway, we performed a suppressor screening based on the recovery of the extreme drought hypersensitive phenotype of the previously characterized *dry2* mutant affected in SQE1 (Posé et al., 2009; see Supplemental Figure 1 online). As a result, four independent mutants were selected and named *sud*, which maintained the reversion of the *dry2* drought hypersensitive phenotype across multiple generations. Identification of the gene affected in the four suppressors indicated that the mutations were allelic (see below), and the mutants were subsequently designated *dry2/sud1-1* to *dry2/sud1-4*.

The recovery of the multiple *dry2* phenotypic defects was further analyzed using the *dry2/sud1-1* and *dry2/sud1-2* alleles. The *dry2/sud1-1* and *dry2/sud1-2* mutants showed a restoration of leaf size and color observed in *dry2* and rendered the mutant shoots undistinguishable from those of the wild type (Figure 1A). This phenotypic recovery of the shoots in the suppressors correlated with the reestablishment of hydrogen peroxide and O_2^- (superoxide) accumulation to wild-type levels (Figure 1B). Since the identification of the suppressors was based on the restoration of the *dry2* extreme drought hypersensitivity, we expected that the defective abscisic acid (ABA) stomatal responses observed in *dry2* would also be restored in the suppressors. As shown in Figure 1C, exogenous application of 20 μM ABA only caused an ~20% reduction in the stomatal conductance of *dry2* compared with the ~80% reduction that occurred in wild-type, *dry2/sud1-1*, and *dry2/sud1-2* plants. In addition, the Pro content in *dry2/sud1-1* and *dry2/sud1-2* was more similar to that of wild-type plants (Figure 1D). These results confirm that the recovery of the *dry2* shoot phenotypes was associated with a restoration of the water relations in the suppressors.

The primary root length of the *dry2/sud1-1* and *dry2/sud1-2* alleles was double than that of *dry2*, reaching ~70% of the wild-type seedlings (Figures 2A and 2B). *dry2/sud1-1* and *dry2/sud1-2* also exhibited a decreased number of lateral roots compared

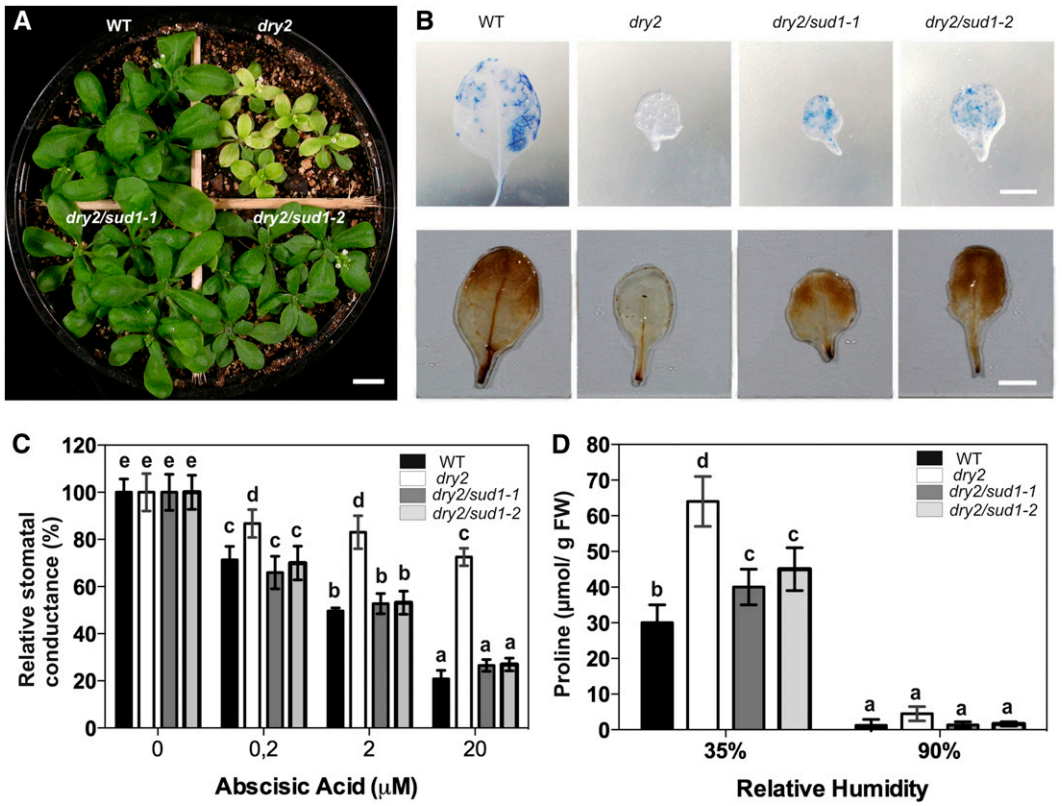

Figure 1. *dry2/sud1-1* and *dry2/sud1-2* Suppress the Shoot Defects of *dry2*.

(A) Shoot phenotype of 3-week-old wild-type (WT), *dry2*, *dry2/sud1-1*, and *dry2/sud1-2* plants grown under standard long-day conditions. Bar = 0.5 cm.
(B) Accumulation of O_2^- (top panel) and hydrogen peroxide (bottom panel) in 3-week-old leaves of the wild type, *dry2*, *dry2/sud1-1*, and *dry2/sud1-2*. Plants were stained with nitroblue tetrazolium (top panel) and DAB (bottom panel). Compared with the wild type, *dry2/sud1-1*, and *dry2/sud1-2*, *dry2* accumulates very low levels of O_2^- and hydrogen peroxide. Bars = 0.5 cm.
(C) Stomatal conductance of the wild type, *dry2*, *dry2/sud1-1*, and *dry2/sud1-2*. The measurements were made 4 h after spraying the indicated ABA concentrations. The suppressors show wild-type stomatal responses to exogenous ABA compared with *dry2*.
(D) Pro content in wild-type, *dry2*, *dry2/sud1-1*, and *dry2/sud1-2* plants grown at 35 and 90% relative humidity. FW, fresh weight.
(C) and **(D)** Mean ± SD, $n = 9$; values with the same letter are not significantly different at $P < 0.05$. The experiments were repeated at least three times with similar results.

with *dry2* (Figures 2A and 2C). The striking defects in root hair length and morphology observed in *dry2* (Posé et al., 2009) were also substantially restored in the suppressors (Figures 2D and 2E). Consistent with the rescue of the root hair growth defects, *dry2/sud1-1* and *dry2/sud1-2* showed wild-type ROS production at the bulge of the root hair tip (Figure 2F), in contrast with the aberrant *dry2* ROS production caused by an ectopic localization of the NADPH oxidase C (AtrbohC) (Posé et al., 2009).

All Four *dry2* Suppressors Harbor Mutations in the *SUD1* Gene

As a first step to determine the gene(s) affected by the *sud* mutations, we crossed *dry2/sud1-1* and *dry2/sud1-2* and performed an allelism test. As shown in Figure 3A, reciprocal crosses rendered progenies with wild-type phenotypes, suggesting that the *sud1-1* and *sud1-2* mutations were allelic. However, F1 plants from the backcross between the suppressors and *dry2* showed an intermediate phenotype, indicating that the mutations were semidominant (Figures 3A and 3B). Based on these results, we could not directly infer whether the *sud1-1* and *sud1-2* mutations were allelic (Koornneef et al., 2006).

Next, we used a combination of map-based cloning and high-throughput sequencing to identify the *sud1-1* mutation. For that purpose, the *dry2* mutant allele (Landsberg *erecta* [L*er*] ecotype) was crossed over seven generations into Columbia-0 (Col-0) ecotype to create an introgression line harboring the *dry2* mutation in the (Col-0) background ($dry2^{Col\text{-}0}$). Molecular markers demonstrated that $dry2^{Col\text{-}0}$ was a near isogenic Col-0 line with the *dry2* mutation, and this line displayed similar phenotypes as the original *dry2* mutant (see Supplemental Figures 2A to 2C online). Since the $dry2^{Col\text{-}0}$ line was a suitable parental line for map based cloning, an F2 population from the cross between *dry2/sud1-1* and $dry2^{Col\text{-}0}$ was generated. Fine-scale map-based cloning delimitated the region harboring the *sud1-1* mutation in chromosome IV between the *AT4G33970* and *AT4G34250* loci

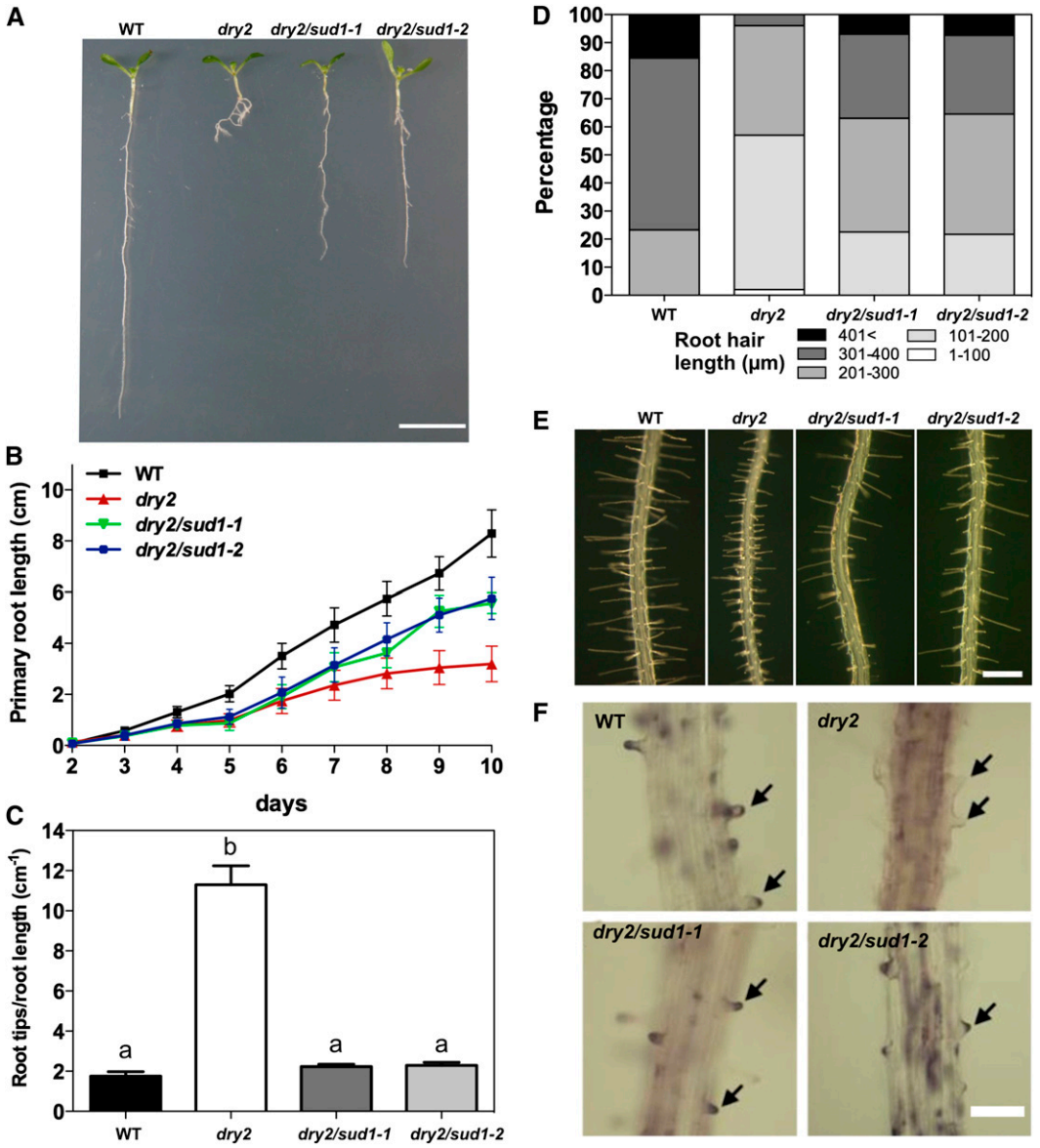

Figure 2. The *dry2/sud1* Mutants Partially Suppress the Root Elongation and Root Hair Growth Defects of the *dry2* Mutant.

(A) Root developmental phenotypes of 10-d-old wild-type (WT), *dry2*, *dry2/sud1-1*, and *dry2/sud1-2* mutant seedlings. Bar = 1 cm.
(B) Primary root growth during a 10-d period for the wild type, *dry2*, *dry2/sud1-1*, and *dry2/sud1-2*. Mean ± SD, $n \geq 30$ roots per genotype.
(C) Root branching index for 10-d-old wild type, *dry2*, *dry2/sud1-1*, and *dry2/sud1-2*. The index was determined by counting the number of lateral root tips per length unit (cm) of primary root. Mean ± SD, $n = 30$ roots counted per genotype. Values with the same letter are not significantly different at $P < 0.05$.
(D) Root hair length distribution in 5-d-old wild-type, *dry2*, *dry2/sud1-1*, and *dry2/sud1-2* ($n \geq 300$ root hairs counted in a total of 30 roots per genotype).
(E) Morphologic root hair phenotype in 5-d-old wild type, *dry2*, *dry2/sud1-1*, and *dry2/sud1-2*. Bar = 500 μm.
(F) ROS staining in 5-d-old roots using DAB. Hydrogen peroxide (arrows) is localized at the tips of wild-type, *dry2/sud1-1*, and *dry2/sud1-2* root hairs, but not in *dry2*. Bar = 200 μm.
[See online article for color version of this figure.]

(see Supplemental Figure 2D online). High-throughput sequencing and analysis of the region containing *sud1-1* determined that the second-site mutation responsible for the *dry2/sud1-1* suppression phenotype was a G-to-A substitution at nucleotide 652 relative to the ATG of the *AT4G34100* gene (hereafter named *SUD1*). This nucleotide change caused a Gly218Arg substitution in the predicted SUD1 amino acid sequence (Figure 3C; see Supplemental Figure 2D online). Rough mapping of the other *sud* mutants using markers linked to *sud1-1* indicated that all four *sud* mutations were located in the same region, and targeted sequencing of the *SUD1* gene identified additional mutations on the three *sud* alleles. Thus, *dry2/sud1-2* caused a Gly360Glu

A

Phenotype of the F1 crosses with the suppressors

♀/♂	*dry2*	*dry2/sud1-1*	*dry2/sud1-2*
dry2	dry2	intermediate	intermediate
dry2/sud1-1	intermediate	WT	WT
dry2/sud1-2	intermediate	WT	WT

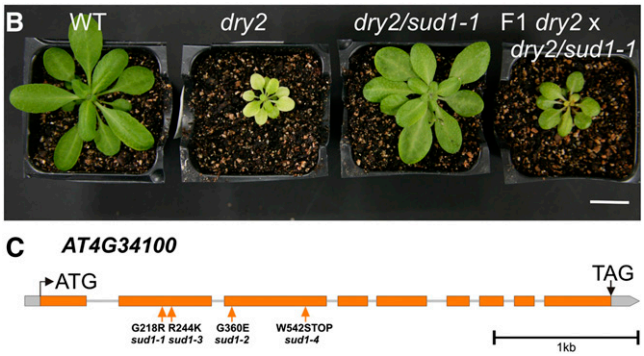

Figure 3. Genetic Analyses of *dry2/sud1-1* and *dry2/sud1-2*.

(A) Visual score of the phenotypes from the F1 of the corresponding crosses. WT, the wild type.

(B) Phenotypes of the wild type, *dry2*, *dry2/sud1-1*, and an F1 plant derived from a backcross between a *dry2/sud1-1* and a *dry2* plant. Bar = 2 cm.

(C) The four suppressor mutations are localized in the *AT4G34100* gene. The intron/exon structure of the gene, the position of the mutations, and the resulting amino acids substitution of the four suppressors are depicted. [See online article for color version of this figure.]

substitution, *dry2/sud1-3* an Arg244Lys substitution, and *dry2/sud1-4* a premature stop codon at position 542 in the predicted SUD1 protein (Figure 3C; see Supplemental Figure 2D online). The identification of four independent *SUD1* mutant alleles in the suppressor screen demonstrates that mutations in the *SUD1* gene are responsible for the phenotypic recovery of the *dry2* defects.

SUD1 Is Homologous to E3 Ubiquitin Ligases from Yeast and Mammals Involved in ERAD

The *Arabidopsis SUD1* locus *AT4G34100* has been recently reported as *ECERIFERUM9*, a gene involved in cuticular wax biosynthesis (Lü et al., 2012), but little is known about the molecular mechanisms underlying SUD1 activity. *SUD1* is predicted to encode a large protein of 1108 amino acids with a molecular mass of ~123 kD. SUD1 contains a Really Interesting New Gene-variant (RING-v) domain (C4HC3 RING-finger domain) near the N terminus (Stone et al., 2005; Lü et al., 2012) and 14 putative TM domains (Lü et al., 2012) (Figure 4A). The SUD1 RING-v domain shares high similarity to that of the E3 ubiquitin ligases TEB4 (57% amino acid identity) and Doa10 (49% amino acid identity). TEB4 and Doa10 are components of the ERAD complex involved in the quality control of ER proteins in human and yeast, respectively (Hassink et al., 2005; Kreft et al., 2006; Kreft and Hochstrasser, 2011). SUD1 also displays a high degree of similarity in an internal conserved segment of ~130 residues called TD (TEB4-Doa10) present in all Doa10 orthologs (Swanson et al., 2001). Thus, the TD domain (TMs 5, 6, and 7) of SUD1 has 45 and 31% amino acid identity to those of TEB4 and Doa10, respectively (Lü et al., 2012).

Next, we generated a topological model for SUD1 using sequence alignments and data from the experimental validation available for the homologous Doa10 (Kreft and Hochstrasser, 2011). For that purpose, we selected multiple SUD1 homologous proteins that complied with the following criteria: (1) the conserved N terminus RING-v domain, (2) the internal conserved TD domain, and (3) at least 10 predicted TM domains (Swanson et al., 2001). As a result of the topological analysis, the N terminus RING-v domain (and hence the putative ligase activity of SUD1) and the C terminus were predicted to face the cytosol (Figure 4), a similar disposition to that of Doa10 (Kreft and Hochstrasser, 2011). This model was also used to locate the putative position of the amino acid residues affected in the different *sud1* mutant alleles. Thus, the mutations in the *sud1-1* and *sud1-2* alleles affected residues located at the transition between a TM domain and a hydrophilic loop. The mutation in *sud1-3* was located in the second cytosolic loop, and the mutation in *sud1-4* produced a premature stop codon at the end of the TM5 domain (Figure 4B).

Additionally, an alignment between SUD1 and SUD1 homologous proteins of several plant species was performed using the plant comparative genomics resource PLAZA database (http://bioinformatics.psb.ugent.be/plaza/; Proost et al., 2010). As shown in Supplemental Figure 3 online, the alignment of *Arabidopsis* SUD1 protein with the most homologous SUD1 proteins from several dicots (*Vitis vinifera*, *Populus trichocarpa*, *Medicago truncatula*, *Lotus japonicus*, and *Glycine max*) and monocots (*Brachypodium distachyon*, *Oryza sativa*, and *Zea mays*) showed striking sequence conservation. From the alignment, we inferred that the amino acid substitutions in all suppressors occurred in conserved residues among monocots and dicots (see Supplemental Figure 3 online).

Suppression of the *dry2* Defects Occurs without Recovery in the Composition of Major Sterols

dry2 and the wild type have similar sterol compositions in shoots but significantly different sterol composition in roots (Posé et al., 2009) (Table 1). Since it has been proposed that the developmental defects in sterol biosynthetic mutants are the result of structural defects due to sterol depletions (Babiychuk et al., 2008; Men et al., 2008), we determined whether the suppression of *dry2* phenotypes was associated with a recovery in sterol content in roots. Sterol profiling using gas chromatography–mass spectrometry analysis was performed separately in the shoots and roots of wild-type, *dry2*, and *dry2/sud1-1* seedlings. As shown in Table 1, wild-type, *dry2*, and *dry2/sud1-1* shoots presented similar bulk sterol compositions. By contrast, the bulk sterol composition in *dry2/sud1-1* roots was similar to that of *dry2* and showed significant differences relative to the wild type. We therefore concluded that the reversion of the *dry2/sud1-1* root defects was not due to a recovery of major sterols to wild-type levels.

The recovery of the *dry2* defects by the *sud1-1* mutation without a recovery of sterol composition was further investigated by analyzing whether *sud1-1* was able to suppress the developmental defects of more severe sterol-deficient mutants. The selected mutants were *cpi1-1*, which causes the loss of function

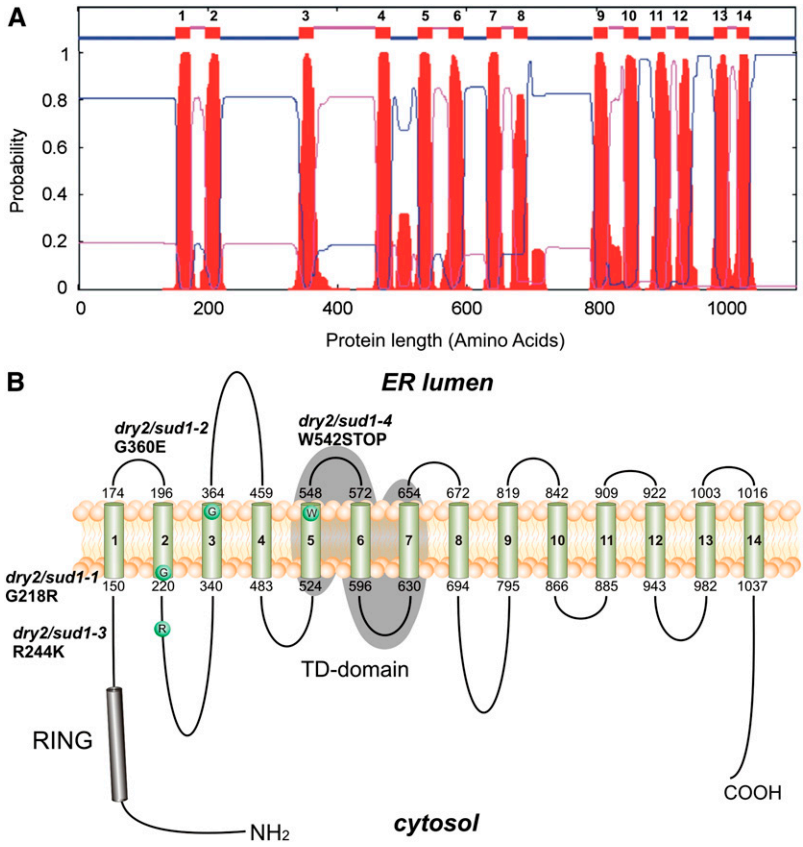

Figure 4. Topology Model for SUD1 Protein.

(A) Hydrophobicity plot of *Arabidopsis* SUD1 predicted by TMHMM2.0. The plot shows the posterior probabilities of inside/outside/TM segments. The 14 TM segments are depicted as numbered small boxes near the top of the figure; lines connected to the bottom edge of these boxes represent cytosolic loops, and those connected to the top edges depict luminal loops.

(B) The 14 TM domains of SUD1 are numbered and represented by cylinders and are the result of the TMHMM2.0 prediction shown in **(A)**. Both protein termini are represented facing the cytosol based on the experimentally determined Doa10 topology (Kreft et al., 2006). The amino acid substitution of a given *sud1* allele is depicted as a circle. Positions of the amino acid substitutions and the protein variants are indicated. The RING domain (residues 68 to 115) at the N terminus is shown as a black cylinder, and the conserved TD domain (residues 524 to 654) is highlighted by gray shading.

[See online article for color version of this figure.]

of the *cyclopropylsterol isomerase gene* (Lovato et al., 2000; Men et al., 2008), and *fackel*, which is mutated in a sterol C-14 reductase (Jang et al., 2000; Schrick et al., 2000). As shown in Supplemental Figure 4 online, no phenotypic recovery was observed when *sud1-1* was introduced in the *cpi1-1* and *fk-x224* mutants. These combined results support the notion that the reversion of the *dry2* phenotype by *sud1* is not concomitant with changes in the sterol content.

A Root-Derived Long-Distance Signal Causes the *dry2* Shoot Phenotypic Defects

Consistent with the identification of SQE1 as the main SQE enzyme in roots and with the sterol profiling results for *dry2* (Rasbery et al., 2007; Posé et al., 2009), we observed a dramatic accumulation of the substrate squalene in roots but not shoots of the *dry2* mutant (Table 1). Interestingly, *dry2/sud1-1* roots showed a significant reduction of squalene relative to *dry2* (Table 1), suggesting that *dry2* root defects could be caused by an accumulation of squalene and/or isoprenoid intermediates upstream of SQE1.

Since *dry2* shoots showed no differences in terms of bulk sterols or squalene accumulations with the wild type, we questioned whether squalene or other isoprenoid intermediates generated in the *dry2* roots could move toward the shoots, causing the observed phenotypes. In order to investigate this possibility, we performed micrografting experiments using wild-type, *dry2*, and *dry2/sud1-1* seedlings. The root and shoot of the grafted plants were genotyped by sequencing the corresponding *DRY2* and *SUD1* alleles. As expected, control grafted plants (i.e., L*er* scion/L*er* rootstock and *dry2* scion/*dry2* rootstock) showed wild-type and *dry2* phenotypes, respectively (Figure 5A). Importantly, *dry2* scion onto both L*er* rootstock (Figure 5A) and dry2/*sud1-1* rootstocks (Figure 5B) showed a wild-type phenotype, suggesting that a root-derived signal was causing the *dry2* shoot defects. Despite multiple attempts, we were unable to obtain a viable graft using wild-type or *sud1-1* scions

Table 1. Mass Spectral Analysis of Sterols and Squalene from the Wild Type, *dry2*, and *dry2/sud1-1*

	Root			Shoot		
Sterol	Wild Type	*dry2*	*dry2/sud1-1*	Wild Type	*dry2*	*dry2/sud1-1*
Cycloartenol	37 ± 6^{a}	104 ± 22^{b}	82 ± 23^{b}	28 ± 2^{a}	28 ± 6^{a}	26 ± 5^{a}
24-Methylenecycloartenol	46 ± 1^{a}	86 ± 12^{b}	102 ± 8^{b}	48 ± 2^{a}	44 ± 3^{a}	47 ± 9^{a}
Isofucosterol	63 ± 4^{a}	41 ± 9^{a}	51 ± 25^{a}	63 ± 3^{a}	69 ± 4^{a}	66 ± 13^{a}
Sitosterol	2579 ± 144^{b}	1518 ± 58^{a}	1617 ± 91^{a}	2234 ± 101^{ab}	2052 ± 34^{a}	2302 ± 148^{b}
Stigmasterol	904 ± 10^{b}	304 ± 53^{a}	317 ± 19^{a}	60 ± 3^{a}	65 ± 13^{a}	69 ± 6^{a}
Campesterol	407 ± 3^{ab}	499 ± 75^{b}	263 ± 107^{a}	422 ± 27^{a}	439 ± 38^{a}	423 ± 50^{a}
Cholesterol	32 ± 12^{a}	18 ± 6^{a}	24 ± 7^{a}	46 ± 4^{a}	45 ± 1^{a}	48 ± 4^{a}
Squalene	10 ± 4^{a}	1206 ± 207^{b}	75 ± 13^{a}	10 ± 2^{a}	15 ± 4^{a}	13 ± 5^{a}

Values are given in μg g^{-1} dry weight. Mean ± SD, n = 3; values with the same letter are not significantly different at $P < 0.05$.

onto *dry2* rootstocks. We therefore could not evaluate the effect of the *dry2* root-derived signal in healthy scions.

sud1 Mutations Suppress *dry2* Root Defects by Downregulating HMGR Activity

It is known that in addition to the accumulation of squalene, the reduction of SQE activity causes a compensatory increase of HMGR activity (Wentzinger et al., 2002; Posé et al., 2009). As shown in Figure 6A, *dry2* roots increased the HMGR activity approximately twofold, while no differences were found in shoots. Importantly, in the roots of *dry2/sud1-1*, the HMGR activity returned to near wild-type levels, whereas in shoots, HMGR activity decreased to ~0.7-fold that in shoots of both the wild type and *dry2* (Figure 6A).

To further investigate whether the reduction of HMGR activity could cause the recovery of the *dry2* roots, we used atorvastatin, a specific inhibitor of HMGR activity. After testing several

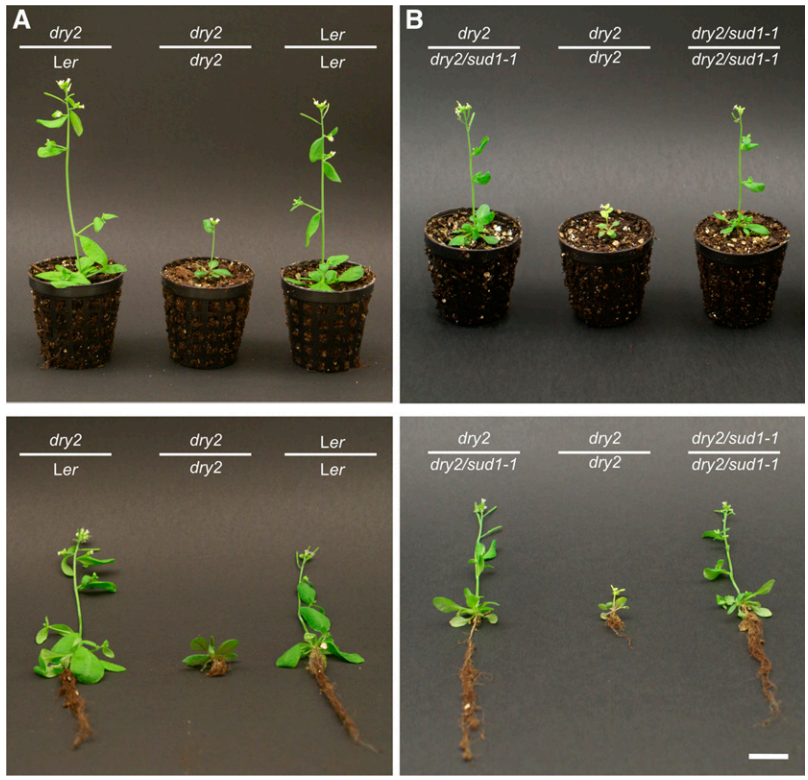

Figure 5. Suppression of *dry2* Shoot (Scion) Defects by Wild-Type and *dry2/sud1-1* Rootstocks.

A total of 20 viable plants per graft combination were analyzed, and a representative plant per combination is depicted after 18 d of growth in soil. Bottom panels show the plants after soil removal to visualize the root phenotype. Bar = 2 cm.

(A) *dry2* shoot (scion) recovers the wild -type phenotype when grafted onto wild-type L*er* rootstock. Self-grafted wild-type (L*er*) and *dry2* were used as controls.

(B) *dry2* shoot (scion) recovers the wild-type phenotype when grafted onto *dry2/sud1-1* rootstock. Self-grafted *dry2/sud1-1* and *dry2* were used as controls.

[See online article for color version of this figure.]

concentrations, we selected 10 nM atorvastatin. As shown in Figure 6B, this concentration did not have apparent effects on wild-type root growth or branching but substantially improved both phenotypes in *dry2*. This result supports the notion that a reduction in HMGR activity in the *dry2*/*sud1-1* suppressor was responsible for the recovery of the *dry2* root phenotypic defects. We next treated wild-type, *dry2*, and *dry2*/*sud1-1* seedlings with MVA, the product of the reaction catalyzed by HMGR. As shown in Figure 6C, a 5 mM MVA treatment caused a mild reduction in wild-type root elongation, while no visible changes were observed in *dry2* roots. However, the same treatment abolished the *sud1-1* suppressive effect of the *dry2* root defects, phenocopying *dry2* roots (Figure 6C). This result indicates that bypassing HMGR activity by adding the product of the HMGR reaction prevents the recovery of the *dry2* phenotype in a *dry2*/*sud1-1* background.

Genetic Analysis of the Regulation of HMGR Activity by SUD1

To further investigate the link between HMGR activity and *SUD1*, the *dry2*/*sud1-1* mutant was crossed with transgenic lines overexpressing the catalytic domain of the HMGR1 (HMGR1-CD) and the short isoform of HMGR1 containing the TM domains (HMGR1S) (see Supplemental Figure 5 online). HMGR1-CD and HMGR1S lines show an ~10-fold and an approximately threefold increase in HMGR activity compared with the wild type, respectively (Manzano et al., 2004). As shown in Figure 7, the enhanced HMGR activity in the wild-type background only caused slight growth inhibition in the HMGR1-CD line and no visible effect in the HMGR1S line (Manzano et al., 2004). By contrast, the HMGR1-CD/*dry2* combination greatly enhanced the growth inhibition defects of *dry2* generating dwarf plants (Figure 7). The HMGR1S/*dry2* combination also showed enhanced growth inhibition compared with *dry2*, but this effect was less drastic than that observed in the HMGR1-CD/*dry2*. In fact, viable seeds were obtained in this genotype, while HMGR1-CD/*dry2* plants died before reaching maturity (Figure 7). These results indicate that the increase in HMGR activity in the presence of a *dry2* mutation accounts for the severity of the observed developmental phenotypes. Importantly, when the *sud1-1* mutation was introduced into HMGR-CD/*dry2* and HMGR1S/*dry2*, there was an important recovery of the defective phenotypes to such an extent that HMGR-CD/*dry2*/*sud1-1* plants were fertile (Figure 7).

Based on these results, we propose a model in which the increase of HMGR activity concomitant to the reduction of SQE1 activity is mainly responsible for the observed developmental phenotypes in the *dry2* background. In this scenario, mutations in the positive regulator of HMGR *SUD1* cause the reversion of the *dry2* developmental defects by decreasing HMGR activity. An obvious question was whether the regulation of HMGR activity by SUD1 was dependent on the presence of the *dry2* mutation. Therefore, the *sud1-1* mutation was segregated from *dry2* by backcrossing *dry2*/*sud1-1* to the wild type. As shown in Figure 8A, the single *sud1-1* mutant did not show any obvious phenotypic difference compared with wild-type plants, except by a glossy-like phenotype in shoots reminiscent of the phenotypes described for the loss-of-function *cer9-1* and *cer9-2* mutants allelic to *sud1* (Lü et al., 2012; see Supplemental Figure 6 online). As shown in Figure 6A, HMGR activity in the *sud1-1* single mutant was ~0.75-fold lower than that of the wild type in both shoots and roots, indicating that *SUD1* is a positive regulator of HMGR activity acting independently of the *dry2* mutation.

Regulation of HMGR Activity by SUD1 Does Not Involve Changes in Protein Content

Because SUD1 contains a RING-v domain putatively involved in ubiquitination (Stone et al., 2005), we used protein gel blot analysis to investigate whether the regulation of HMGR activity mediated by SUD1 involves changes in HMGR protein content. The immunospecific antibodies used in the analysis were raised against the catalytic domain of HMGR1 (Manzano et al., 2004; Leivar et al., 2005). As shown in Figure 8B, the analysis of HMGR protein content in root samples revealed two bands of ~63 and 69 kD, corresponding to the HMGR1S and HMGR1L isoforms, respectively, whereas in shoot samples, only the 63-kD protein band was detected. In both cases, no significant differences in HMGR protein content among the wild type, *dry2*, *dry2*/*sud1-1*, and *sud1-1* were observed (Figure 8B). This result, together with results from previous pharmacological studies (Wentzinger et al., 2002; Nieto et al., 2009), indicates that the variations in HMGR activity in the different genetic backgrounds occur without changes in the total HMGR protein content.

DISCUSSION

Mutations in the sterol biosynthetic *SQE1* gene produce multiple developmental defects, but in contrast with null alleles of *SQE1* (Rasbery et al., 2007), the hypomorphic *sqe1-5* allele is fully fertile (Posé et al., 2009). This characteristic lends itself to the use of *dry2*/*sqe1-5* as a genetic tool to identify processes that otherwise would be concealed. To find components regulating isoprenoid biosynthesis and/or signaling in *Arabidopsis*, we performed genetic screening for suppressors of *dry2*. Here, we report the analysis of four suppressors and show that all mutations affect the *At4g34100* gene encoding a protein with a RING-v domain, found in ubiquitin E3 ligases, subsequently named SUD1. Based on phylogenetic and structural similarities, it is proposed that SUD1 is an *Arabidopsis* orthologous protein of yeast Doa10 and mammalian TEB4, which are involved in the ERAD-C pathway. Our physiological, molecular, biochemical, and genetic analyses strongly support that *sud1* recovers the *dry2* defects through the reversion of the enhanced HMGR activity of *dry2* to wild-type levels. Thus, our study uncovers *SUD1* as a regulator of HMGR activity in the plant isoprenoid biosynthetic pathway.

The Accumulation of an MVA-Derived Signal in Roots Causes the *dry2* Phenotypes

Despite its dramatic phenotypic defects, sterol analysis of *dry2* showed only moderate changes in major bulk sterols in roots and no significant changes in shoots, compared with the wild type. Interestingly, sterol analysis of *dry2*/*sud1-1* roots revealed a similar composition to that of *dry2*, indicating that the *dry2*

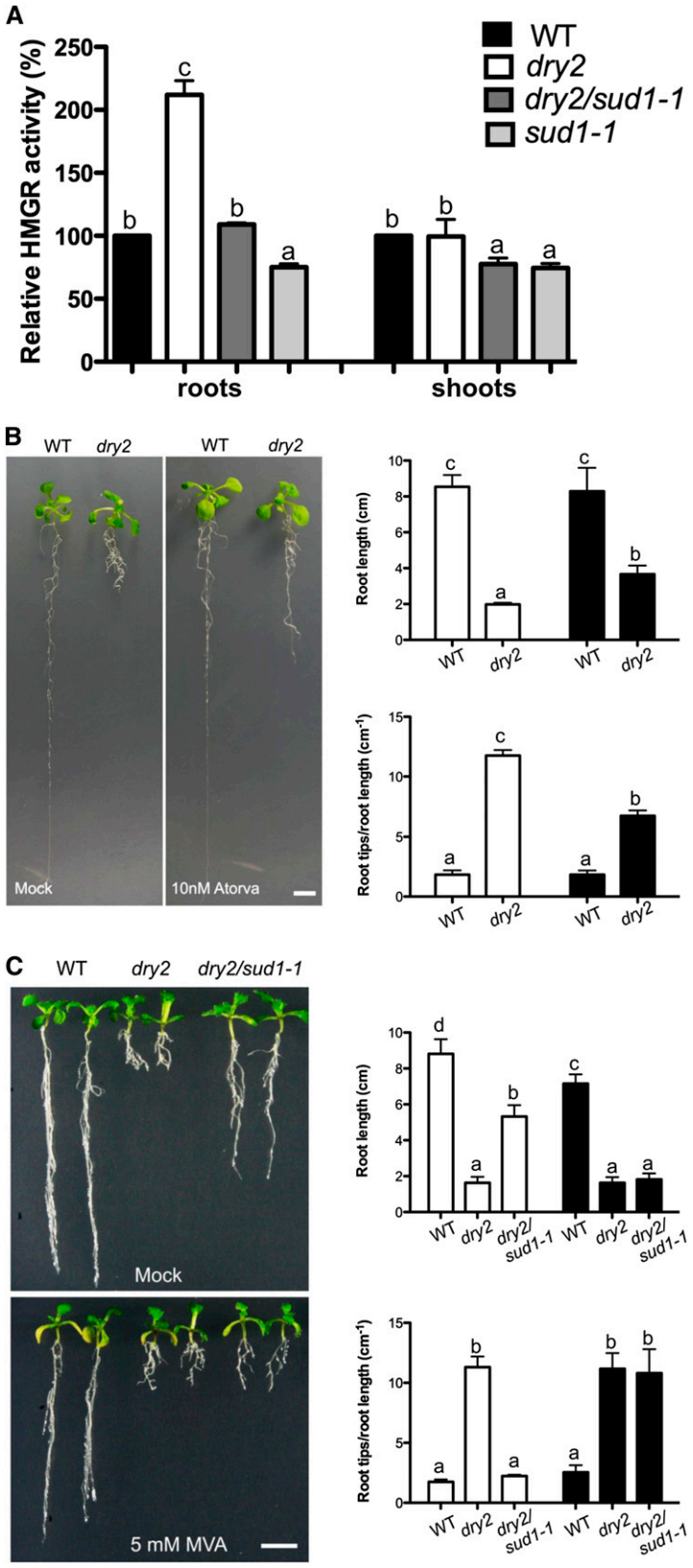

Figure 6. HMGR Activity Changes Correlate with the Phenotypes Observed in *dry2* and *dry2/sud1-1*.

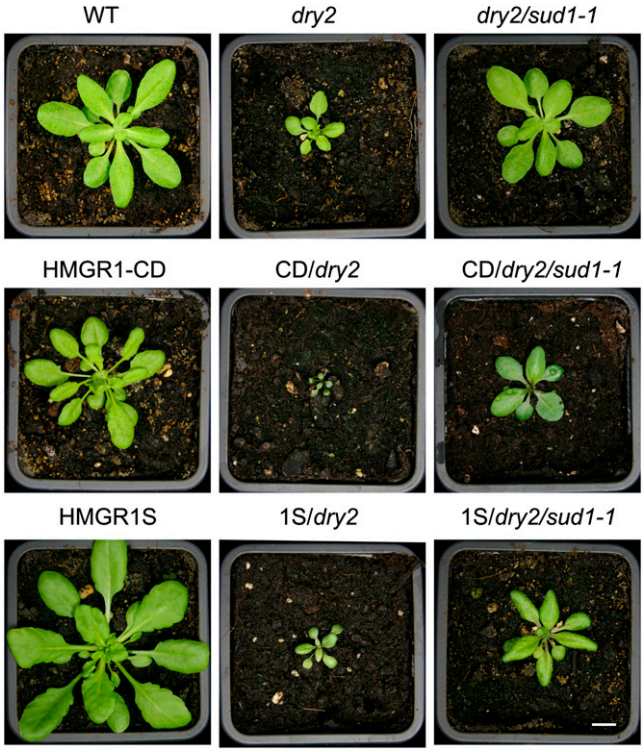

Figure 7. Phenotypic Analysis of Plants Overexpressing *HMGR1S* and *HMGR1-CD* in *dry2* and *dry2/sud1-1* Backgrounds.

Wild-type (WT), *dry2*, and *dry2/sud1-1* plants are in the L*er* background ecotype. The transgenic HMGR1-CD or HMGR1S plants are in Col glabrous background. The resulting F2 from the crosses are Col-L*er* hybrids. Plants were grown for 3 weeks in soil under long-day conditions. All plants were fertile with the exception of CD/*dry2* plants. Bar = 1 cm. [See online article for color version of this figure.]

phenotypes cannot simply be explained by structural defects caused by the reduction in bulk sterols. Moreover, *dry2* shoots display wild-type characteristics when grafted onto wild-type rootstocks, suggesting that a toxic mobile signal that originated in the *dry2* roots is responsible for the observed *dry2* shoot phenotypes.

Although it is tempting to speculate that the squalene accumulated in *dry2* roots is the mobile signal responsible for the phenotypes, we argue against this notion because plants deal with excess endogenously produced or exogenously added squalene by storing it as remobilizable cytosolic lipid droplets without obvious phenotypic defects (Wentzinger et al., 2002; Bouvier-Navé et al., 2010). Thus, we propose an alternative model whereby the accumulation of toxic intermediates, or derivatives acting upstream of squalene, is responsible for the observed *dry2* developmental phenotypes. In fact, three independent experiments, including (1) the inhibition of HMGR with atorvastatin that partially improved the *dry2* root defects, (2) the HMGR bypass with MVA that caused *dry2/sud1-1* (but not the wild type) to phenocopy *dry2*, and (3) the overexpression of HMGR that enhanced the *dry2* phenotypes, suggest that the *dry2* mobile signal(s) is not only triggered by the reduction of SQE1 activity but also by the concomitant upregulation of HMGR activity.

Supporting our model, the presence of toxic MVA-derived intermediates associated with HMGR activity changes has been reported in Insig double knockout mice that show developmental defects linked to enhanced HMGR activity (Engelking et al., 2006). As was true for *dry2*, the developmental defects of the mice were ameliorated with the use of HMGR inhibitors (Engelking et al., 2006). Interestingly, the Insig knockout mice are not an isolated example. Nonsterol MVA-derived compounds upstream of squalene have been linked to the regulation of HMGR protein content in mammals, yeast, and plants. Thus, the degradation of mammalian HMGR is accelerated by the addition of farnesol, geranylgeraniol, and its precursor geranylgeranyl diphosphate (Correll et al., 1994; Meigs et al., 1996; Räikkönen et al., 2010). geranylgeranyl diphosphate is also known to regulate the degradation of HMGR2p in yeast (Garza et al., 2009). Surprisingly, the effect of farnesol on plant HMGR activity seems to be different from that in mammals because the addition of subtoxic concentrations of farnesol to tobacco Bright Yellow-2 cells had a drastically stimulatory effect on HMGR activity (Hemmerlin and Bach, 2000).

Despite the similarities in the regulation of HMGR by a nonsterol MVA-derived molecule in different species, the mechanisms that regulate HMGR activity in *Arabidopsis* seem to operate at a different level from those in yeast and animals. Thus, our study and a previous report (Nieto et al., 2009) have shown that both the genetic and pharmacological block of *Arabidopsis* SQE activity leads to upregulation of HMGR activity without changing HMGR protein amounts, while in yeast and animals, HMGR activity depends on protein stability.

Figure 6. (continued).

(A) HMGR activity measurement in roots and shoots of 15-d-old wild-type (WT), *dry2*, *dry2/sud1-1*, and *sud1-1* seedlings (mean ± SD, $n = 3$; each measurement corresponds to a pool of ≥100 seedlings). Values with the same letter are not significantly different at $P < 0.05$. The experiment was repeated at least three times with similar results.

(B) Inhibition of HMGR activity partially recovers *dry2* roots defects. Wild-type and *dry2* seeds were germinated and grown on MS plates for 4 d. Seedlings were then transferred to MS supplemented with 10 nM of the HMGR inhibitor atorvastatin and grown for additional 2 weeks (mean ± SD, $n = 30$; values with the same letter are not significantly different at $P < 0.05$). The experiment was repeated three times with similar results. Bar = 1 cm.

(C) *dry2/sud1-1* roots phenocopy *dry2* in the presence of MVA. The wild type, *dry2*, and *dry2/sud1-1* were germinated and grown on MS plates for 4 d. Seedlings were then transferred to MS medium supplemented with MVA and grown for two additional weeks (mean ± SD, $n = 30$; values with the same letter are not significantly different at $P < 0.05$). The experiment was repeated three times with similar results. Bar = 1 cm.

[See online article for color version of this figure.]

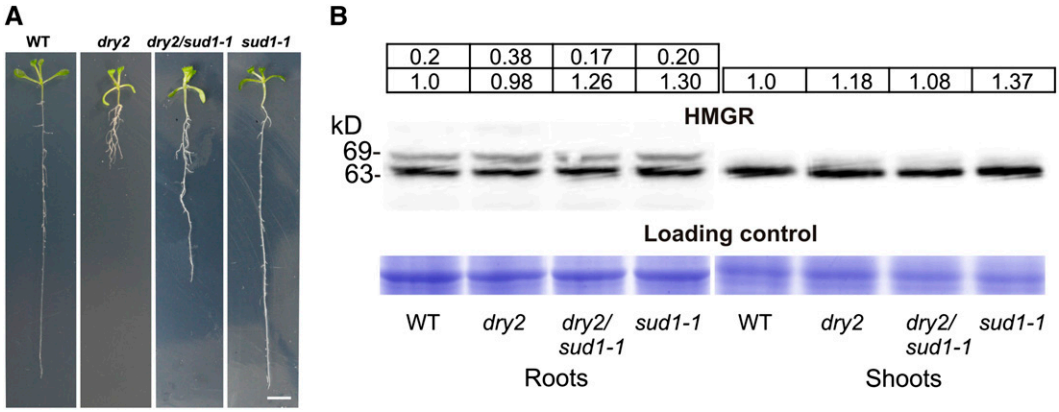

Figure 8. *sud1-1* Mutation Produces No Visible Phenotype and No Changes in HMGR Protein Content.

(A) Phenotype of wild-type (WT), *dry2*, *dry2/sud1-1*, and *sud1-1* seedlings grown for 15 d on MS medium under long-day conditions. Bar = 1 cm.
(B) Protein gel blot analysis of HMGR protein in 15-d-old roots and shoots of the wild type, *dry2*, *dry2/sud1-1*, and *sud1-1*. Intensities of the HMGR protein bands (top panel) and the Coomassie blue–stained gel (bottom panel) were quantified using ImageJ software (http://rsb.info.nih.gov/ij). The normalized HMGR protein levels expressed as relative abundance to the amount of the HMGR1S isoform in wild-type plants (arbitrarily set at 1) is shown at the top of each lane. Image shows the results from one representative experiment. Four independent experiments were performed with similar results. [See online article for color version of this figure.]

Structural Characteristics of SUD1

All *sud1* alleles show a similar phenotypic recovery of *dry2* phenotypes, including *sud1-4*, which is caused by a premature stop codon at the fifth TM domain. The *sud1* alleles also show a glossy-like phenotype in leaves reminiscent of the *cer9* mutants in the same locus. Because *cer9* has been reported to be a loss-of-function mutant (Rashotte et al., 2004; Lü et al., 2012), and the premature stop codon is much more downstream in *cer9-2* than in *sud1-4*, we presume that *sud1* are also loss-of-function alleles. Interestingly, the *cer9* alleles are recessive while all *sud1* alleles are semidominant with respect to the *dry2* mutation, which suggests that *SUD1* regulation of HMGR activity is dose dependent. Thus, the heterozygous, *SUD1/sud1* genotype is unable to produce enough SUD1 protein to fully reproduce the *dry2* phenotypes.

The phylogenetic analysis and the structural features of SUD1 suggest that this protein might function as one ortholog of yeast Doa10 and human TEB4 in *Arabidopsis* (Carvalho et al., 2006; Kreft et al., 2006; Kreft and Hochstrasser, 2011); these proteins are involved in the quality control that degrades misfolded ER proteins (Swanson et al., 2001). However, despite multiple attempts, we failed to complement the yeast *doa10* mutant with SUD1 because this protein is highly unstable in yeast. This result is not entirely surprising because efforts to perform complementation of yeast *doa10* with TEB4 have also been unsuccessful despite the fact that yeast Doa10 and human TEB4 are orthologous proteins (Kreft et al., 2006).

When we analyze SUD1 plant homologs, we find a striking conservation of SUD1 sequence with homologous proteins from dicots and monocots. Indeed, amino acid substitutions in all suppressors occur in plant conserved residues. Thus, *sud1-1* and *sud1-2* result in Gly218Arg and Gly360Glu substitutions that change small nonpolar residues for basic and acidic residues, respectively. Interestingly, both residues are located at the transition between a TM segment and a hydrophylic loop. Interruption of TM helices by a short nonhelical segment containing Pro, Gly, and/or Ser residues has also been observed in many classes of transporters, including amino acid antiporters (Gao et al., 2009), neurotransmitter-sodium symporters (Yamashita et al., 2005), and sodium-independent transporters (Schulze et al., 2010). Interruption of helical structures exposes main-chain carbonyl oxygen and nitrogen atoms for hydrogen bonding and ion coordination, aspects that are essential for proper function (Yamashita et al., 2005). The mutation in *sud1-3* results in the Arg244Lys substitution. These two amino acids are chemically related, and it would be expected that its substitution did not cause important changes. However, phylogenetically distant plant species, such as monocots and dicots, maintain a conserved Arg around position 244, suggesting an important role for this specific residue in SUD1 function.

Regulation of HMGR Activity by SUD1

A wealth of information about ERAD comes from yeast and mammals (Vembar and Brodsky, 2008; Smith et al., 2011). The HRD pathway (ERAD-L and ERAD-M) is involved in the degradation of misfolded ER-luminal and intramembrane domains; *HRD* genes were identified in a genetic screening for regulators of HMGR degradation (hence the name HRD, for HMGR reductase degradation) (Hampton et al., 1996). The finding that feedback regulation of sterol synthesis in mammalian and yeast cells uses the ERAD machinery (Hampton, 2002) illustrates cooption of the basic quality control mechanism for regulatory processes and reveals potential functions in cell-to-cell signaling. ERAD-regulated HMGR proteins, such as those from yeast and mammals, contain the known sterol sensing domain motif consisting of five consecutive TM spans (Goldstein et al., 2006; Theesfeld et al., 2011). However, HMGR from plants contain two predicted TM domains (see Supplemental Figure 5 online)

(Campos and Boronat, 1995), therefore lacking any potential sterol sensing domain motif. Surprisingly, following a non-targeted screening for plant HMGR regulators, we identified SUD1, a likely ERAD component. Our first explanation for this was that HMGR stability was regulated by ERAD, either directly by SUD1 or through a compensatory increase of the HRD pathway in *sud1* mutants. However, protein gel blot analyses indicated that SUD1 did not exert its function by regulating HMGR proteins levels. Because SUD1 likely encodes an E3 ubiquitin ligase, another plausible explanation is that a negative regulator of HMGR is being degraded in a SUD1-dependent manner in *dry2*, so the loss of SUD1 function would impair this degradation, leading to the recovery of HMGR activity to wild-type levels.

Transcriptional versus Translational Regulation of HMGR

It has been proposed that major changes in HMGR activity in plants would be determined at the transcriptional level, whereas posttranslational control would allow a finer and faster adjustment (Chappell, 1995). Whereas transcriptional modulation of HMGR has been demonstrated in many plant systems, evidence for mechanisms regulating HMGR activity at the posttranslational level is scarce. Thus, Nieto et al. (2009) have shown that metabolic perturbations by enhancing or depleting the flux through the sterol pathway in *Arabidopsis* causes a compensatory response in HMGR activity, without changes in transcript or protein levels, and Flores-Pérez et al. (2010) reported that the inactivation of the *Arabidopsis* WD protein PRL1 leads to reduced HMGR activity with no changes in transcript and protein levels. This effect could be related to the ability of PRL1 to interact and inhibit the activity of the *Arabidopsis* SNF1-related protein kinases (SnRK1) AKIN10 and AKIN11 (Bhalerao et al., 1999), presumably targeting them for ubiquitination and proteasomal degradation (Lee et al., 2008). Since plant SnRK1 phosphorylates and inactivates HMGR (Dale et al., 1995; Sugden et al., 1999), the loss of PRL1 function would result in increased SnRK1 activity followed by HMGR phosphorylation and the subsequent reduction of HMGR activity. It has also been demonstrated that HMGR activity is negatively regulated by PP2A-mediated dephosphorylation (Leivar et al., 2011). Therefore, SnRK1 and/or PP2A, regulators of *Arabidopsis* HMGR activity, are candidates to act as mediators of SUD1 regulation of HMGR activity. An alternative possibility is that SUD1 might produce the direct monoubiquitination of HMGR, thereby increasing its activity, as has been reported for other proteins (Schnell and Hicke, 2003).

Overall, using genetic, physiological, biochemical, and molecular approaches, we show that SUD1, a likely component of the *Arabidopsis* ERAD-C pathway, is a positive regulator of HMGR activity. Future research should help clarify the mechanistic basis for the ERAD regulation of HMGR activity in plants and what signals are implicated in this regulation.

METHODS

Plant Material and Growth Conditions

Unless stated otherwise, the *Arabidopsis thaliana* plants used in this study were either grown on soil or in Petri dishes using an environmental chamber set for long-day lighting conditions (16 h light/8 h dark) and a temperature of 22°C. For in vitro assays, surface-sterilized and cold-stratified *Arabidopsis* seeds were sown onto Murashige and Skoog (MS) phytagel-solidified medium (MS salts, 30 g L^{-1} Suc, and 7 g L^{-1} phytagel [Sigma-Aldrich], pH 5.7). For chemical treatments, the appropriate amounts of filter sterilized chemical stock solutions were added to cooled autoclaved growth medium. The *dry2* (Posé et al., 2009), *cpi1-1* (Schrick et al., 2000), and *fk-x224* (Men et al., 2008) mutants and the HMGR1-CD and HMGR1S overexpressing lines (Manzano et al., 2004) have been previously described.

Genetic Screen for Second-Site Suppressor Mutations of *dry2*

The *dry2* seeds were mutagenized by imbibition in 75 mM ethyl methanesulfonate (Sigma-Aldrich) for 4 h at room temperature. After washing thoroughly with water for complete ethyl methanesulfonate removal, the mutagenized seeds (M1) were sown on soil and grown under high humidity conditions. The M2 seeds were harvested as 131 independent pools (each pool corresponding to 50 M1 plants). For the identification of *dry2* suppressors, the M2 seeds were grown on soil under low watering conditions. Suppressors with enhanced drought tolerance compared with *dry2* plants were visually identified and selected for further analysis. The *SQE1-DRY2* gene of each candidate suppressor was amplified by PCR using *DRY2*-specific primers and sequenced in order to confirm the presence of the *dry2* mutation as described by Posé et al. (2009). The primers sequences for genotyping were DRY2 SEQ F, 5′-ATTGTTCTCGGTTGGGTGAG-3′, and DRY2 SEQ R, 5′-GATTGCAGTTCTCTAGGACCAA-3′, and internal primer to sequence DRY2 SEQ2, 5′-TCAAAGAATGCGGGAGAAAG-3′.

Detection of ROS

Hydrogen peroxide was visually detected in leaves using the 3,3′-diaminobenzidine (DAB; Sigma-Aldrich) substrate as described previously (Orozco-Cardenas and Ryan, 1999). DAB was also used for in situ detection of hydrogen peroxide in roots from seedlings grown on phytagel-solidified medium (Carol et al., 2005). For in situ detection of superoxide in leaves, the nitroblue tetrazolium (NBT Color Development Substrate; Promega) staining method (Jabs et al., 1996) was used. In all cases, stained leaves were imaged under dark-field illumination using a Leica MZ FLII stereomicroscope.

Whole-Plant Stomatal Conductance and Determination of Pro Content

Leaf stomatal conductance to water vapor was measured in 25-d-old leaves grown under short-day lighting conditions (8 h light/16 h dark) using a Leaf Porometer Model SC-1 (Decagon Services). Measurements were performed after spraying the leaves with 0, 0.2, 2, or 20 μM of ABA (Sigma-Aldrich) dissolved in a 0.1% Tween 20 solution. Pro was extracted and quantified as described previously (Borsani et al., 2002).

Root Measurements

Root measurements were performed according to the procedure described by Posé et al. (2009). Briefly, seeds were grown vertically on phytagel-solidified MS medium for 5 and 10 d for roots hair and root elongation measurements, respectively. For root elongation assays, primary root length pictures were taken daily using a Nikon Coolpix 4500 camera attached to a MZ FLII stereomicroscope (Leica). Quantitative measurements were made using Image J software (http://rsb.info.nih.gov/ij/). Root branching was determined by counting the number of root tips per length unit (cm) of primary root. Root hair length was measured in the differentiation zone as described by Posé et al. (2009).

Identification of the *sud1-1* Suppressor Mutation

The *dry2* mutant in the L*er* background was crossed into the Col-0 ecotype for seven generations to generate a nearly isogenic *dry2*$^{Col-0}$ line for map-based cloning. An F2 mapping population was created from a cross between the *dry2/sud1-1* (L*er*) and the introgressed *dry2*$^{Col-0}$ lines. A total of 120 F2 plants displaying the suppression phenotypes conferred by the *dry2/sud1-1* mutations were used for rough mapping. For fine mapping, a total of 2400 chromosomes were analyzed to locate the *SUD1* locus in a 117-kb region at the bottom of chromosome IV with 36 candidate genes. All information regarding the genetic markers used in the map-based cloning was obtained from The Arabidopsis Information Resource (http://www.Arabidopsis.org/). The entire genome of *dry2/sud1-1* was sequenced using high-throughput sequencing with the Illumina platform. Reads were filtered with Fastx-Toolkit software (http://hannonlab.cshl.edu/fastx_toolkit/index.html) and mapped with the *Arabidopsis* genome sequence version TAIR10 using the Burrows-Wheeler Alignment Tool (Li and Durbin, 2009). Polymorphisms for the 117-kb candidate region were analyzed with Samtools and Bcftools using regions with at least 5× depth coverage (Li et al., 2009) and filtered using the sequence information for the L*er* ecotype available at 1001 Genomes (http://1001genomes.org/). After filtering, two nonsynonymous mutations in the *AT4G34100* and *AT4G34135* loci were identified. The identification of four independent suppressor alleles with mutations in the *AT4G34100* locus confirmed the identity of the *AT4G34100* locus as *SUD1*.

Informatic Tools Used for Functional Characterization of SUD1

The InterPro database (http://www.ebi.ac.uk/Tools/pfa/iprscan/) was used to search for conserved domains of SUD1 protein. The National Center for Biotechnology Information BLASTp tool (http://blast.ncbi.nlm.nih.gov/Blast.cgi?PAGE=Proteins) was used to identify putative SUD1 orthologs using the predicted proteome from *Saccharomyces cerevisiae* (taxid4932), *Homo sapiens* (taxid9606), *Mus musculus* (taxid10090), *Drosophila melanogaster* (taxid7227), and *Caenorhabditis elegans* (taxid6239).

The TMHMM2.0 program (www.cbs.dtu.dk/services/TMHMM/) was used to predict the putative TM domain topology of SUD1 based on the hydrophobicity plot (Krogh et al., 2001). The plant comparative genomics resource PLAZA (http://bioinformatics.psb.ugent.be/plaza/) was used to search for SUD1 homologous protein sequences in different plant species (Proost et al., 2010). Protein sequence alignment of *Arabidopsis* SUD1 with homologous proteins from other plant species was performed with the software ClustalW2 available online from the European Bioinformatics Institute (http://www.ebi.ac.uk/Tools/msa/clustalw2/). Default values were used for all parameters, including Gonnet protein weight matrix, gap open of 10, gap extension of 0.20, gap distance of 5, no end gaps, should read: no iteration, numiter of 1, and clustering neighbor-joining no iteration, numiter of 1, and clustering neighbor-joining (Gonnet et al., 1992).

Sterol and Squalene Analysis and Determination of HMGR Activity

Fifteen-day-old seedlings grown in phytagel-solidified MS medium were used for sterol, squalene, and HMGR activity measurements. A pool of ≥100 seedlings per genotype was used per each measurement. Since HMGR activity and isoprenoid biosynthesis are regulated by light conditions (Learned, 1996; Rodríguez-Concepción et al., 2004), shoot and roots were collected and measured separately at 3 h from the start of the light period. Quantification of total sterol content and determination of sterol profiles were performed as previously reported (Masferrer et al., 2002). HMGR activity was assayed as described (Nieto et al., 2009). In our assays, one unit of HMGR activity is defined as the amount of enzyme that converts 1 pM of 3-hydroxy-3-methylglutaryl CoA into MVA per min and mg of protein at 37°C.

Arabidopsis Grafting

Four-day-old seedlings grown vertically were transferred to a 0.22-μm sterile filter (Millipore) in contact with half-strength MS medium containing 0.6% (w/v) phytagel (Sigma-Aldrich). After 3 d, seedlings were grafted in a wedge graft (Y shape) under sterile conditions, as described by Turnbull et al. (2002). Afterwards, the grafted plants were grown for seven additional days under humid conditions. Successful grafts were transferred to soil, and the grafting unions were confirmed by sequencing analysis of the *dry2* mutant allele of shoots and roots as described above.

Determination of HMGR Protein Levels

HMGR protein levels were determined by immunoblot analysis using a rabbit polyclonal antibody raised against the catalytic domain of *Arabidopsis* HMGR1 (Manzano et al., 2004; Leivar et al., 2005). The antibody was used at 1:1000 dilution, and the secondary antibody (horseradish peroxidase anti-rabbit IgG; Sigma-Aldrich) was diluted at 1:14,000. For immunoblot analysis, total root and shoot protein were loaded onto 10% acrylamide SDS gels. Immunoblot images were developed with Advanced ECL (GE Healthcare) and exposed to an x-ray film for 30 s to 1 min. Coomassie Brilliant Blue staining was used to confirm equal loading.

Statistical Analysis

Statistical analysis was performed using the Statgraphic Centurion program (Statpoint Technologies). The significance of differences was determined by analysis of variance (for three or more samples) or a *t* test (for two samples).

Accession Numbers

Arabidopsis Genome Initiative locus identifiers for the genes mentioned in this article are as follows: SQE1 (At1g58440), SUD1 (At4g34100), CPI1 (At5g50375), FK (At3g52940), and HMGR1 (At1g76490).

Supplemental Data

The following materials are available in the online version of this article.

Supplemental Figure 1. Identification of Suppressor Lines Recovering the *dry2* Drought Hypersensitivity.

Supplemental Figure 2. Map-Based Cloning of *sud1-1*.

Supplemental Figure 3. Protein Sequence Alignment of SUD1 with Homologs from Other Plant Species.

Supplemental Figure 4. The *sud1-1* Mutation Does Not Improve the Phenotypic Defects of the Sterol Biosynthesis Mutants *cpi1-1* and *fk-x224*.

Supplemental Figure 5. Schematic Representation of the HMGR Protein Versions Overexpressed in the HMGR1S and HMGR1-CD Transgenic Lines.

Supplemental Figure 6. *sud1-1* Leaves but Not the Wild Type Show Glossy-Like Appearance.

ACKNOWLEDGMENTS

We thank Pedro Carvalho for helpful suggestions and Colin Turnbull for advice on grafting experiments. This work was supported by grants from Ministerio de Ciencia e Innovación (cofinanced by the European Regional Development Fund) to M.A.B. (BIO2011-23859 and CSD2007-00057), A.F. (BIO2009-06984 and CSD2007-00036), and O.B. from Universidad

de la República-Comisión Sectorial de Investigación Científica (Grupo 418). V.G.D. was supported by a Formación del Personal Investigador fellowship from Ministerio de Educación y Ciencia (BIO2005-04733), and V.A.-S. was supported by Fundação para a Ciência e a Tecnologia (FCT) (Grant SFRH/BD/38583/2007).

AUTHOR CONTRIBUTIONS

V.G.D. and V.A.-S. performed the physiological, biochemical, and genetic experiments. D.P. identified the suppressors and performed an initial characterization. M.A. performed sterols and squalene analysis and HMGR activity measurements. A.B. conducted the genomic analysis for *SUD1* identification. H.A. performed the ROS analyses. A.E. performed genetic crosses for *SUD1* identification. O.B. designed and performed the atorvastatin experiments. V.G.D., A.R., V.V., R.M.T., and M.A.B. designed the research. V.G.D.,V.A.-S., A.R., A.F., and M.A.B. wrote the article.

Received December 18, 2012; revised January 23, 2013; accepted January 29, 2013; published February 12, 2013.

REFERENCES

Babiychuk, E., Bouvier-Navé, P., Compagnon, V., Suzuki, M., Muranaka, T., Van Montagu, M., Kushnir, S., and Schaller, H. (2008). Allelic mutant series reveal distinct functions for *Arabidopsis* cycloartenol synthase 1 in cell viability and plastid biogenesis. Proc. Natl. Acad. Sci. USA **105:** 3163–3168.

Benveniste, P. (2004). Biosynthesis and accumulation of sterols. Annu. Rev. Plant Biol. **55:** 429–457.

Bhalerao, R.P., Salchert, K., Bakó, L., Okrész, L., Szabados, L., Muranaka, T., Machida, Y., Schell, J., and Koncz, C. (1999). Regulatory interaction of PRL1 WD protein with *Arabidopsis* SNF1-like protein kinases. Proc. Natl. Acad. Sci. USA **96:** 5322–5327.

Borsani, O., Cuartero, J., Valpuesta, V., and Botella, M.A. (2002). Tomato tos1 mutation identifies a gene essential for osmotic tolerance and abscisic acid sensitivity. Plant J. **32:** 905–914.

Boutté, Y., and Grebe, M. (2009). Cellular processes relying on sterol function in plants. Curr. Opin. Plant Biol. **12:** 705–713.

Bouvier, F., Rahier, A., and Camara, B. (2005). Biogenesis, molecular regulation and function of plant isoprenoids. Prog. Lipid Res. **44:** 357–429.

Bouvier-Navé, P., Berna, A., Noiriel, A., Compagnon, V., Carlsson, A.S., Banas, A., Stymne, S., and Schaller, H. (2010). Involvement of the phospholipid sterol acyltransferase1 in plant sterol homeostasis and leaf senescence. Plant Physiol. **152:** 107–119.

Brodersen, P., Sakvarelidze-Achard, L., Schaller, H., Khafif, M., Schott, G., Bendahmane, A., and Voinnet, O. (2012). Isoprenoid biosynthesis is required for miRNA function and affects membrane association of ARGONAUTE 1 in *Arabidopsis*. Proc. Natl. Acad. Sci. USA **109:** 1778–1783.

Campos, N., and Boronat, A. (1995). Targeting and topology in the membrane of plant 3-hydroxy-3-methylglutaryl coenzyme A reductase. Plant Cell **7:** 2163–2174.

Carland, F., Fujioka, S., and Nelson, T. (2010). The sterol methyltransferases SMT1, SMT2, and SMT3 influence *Arabidopsis* development through nonbrassinosteroid products. Plant Physiol. **153:** 741–756.

Carol, R.J., Takeda, S., Linstead, P., Durrant, M.C., Kakesova, H., Derbyshire, P., Drea, S., Zarsky, V., and Dolan, L. (2005). A RhoGDP dissociation inhibitor spatially regulates growth in root hair cells. Nature **438:** 1013–1016.

Carvalho, P., Goder, V., and Rapoport, T.A. (2006). Distinct ubiquitin-ligase complexes define convergent pathways for the degradation of ER proteins. Cell **126:** 361–373.

Chappell, J. (1995). The biochemistry and molecular biology of isoprenoid metabolism. Plant Physiol. **107:** 1–6.

Clouse, S. (2002). *Arabidopsis* mutants reveal multiple roles for sterols in plant development. Plant Cell **14:** 1995–2000.

Correll, C.C., Ng, L., and Edwards, P.A. (1994). Identification of farnesol as the non-sterol derivative of mevalonic acid required for the accelerated degradation of 3-hydroxy-3-methylglutaryl-coenzyme A reductase. J. Biol. Chem. **269:** 17390–17393.

Dale, S., Arró, M., Becerra, B., Morrice, N.G., Boronat, A., Hardie, D.G., and Ferrer, A. (1995). Bacterial expression of the catalytic domain of 3-hydroxy-3-methylglutaryl-CoA reductase (isoform HMGR1) from *Arabidopsis thaliana*, and its inactivation by phosphorylation at Ser577 by *Brassica oleracea* 3-hydroxy-3-methylglutaryl-CoA reductase kinase. Eur. J. Biochem. **233:** 506–513.

Eisenreich, W., Rohdich, F., and Bacher, A. (2001). Deoxyxylulose phosphate pathway to terpenoids. Trends Plant Sci. **6:** 78–84.

Engelking, L.J., Evers, B.M., Richardson, J.A., Goldstein, J.L., Brown, M.S., and Liang, G. (2006). Severe facial clefting in Insig-deficient mouse embryos caused by sterol accumulation and reversed by lovastatin. J. Clin. Invest. **116:** 2356–2365.

Enjuto, M., Balcells, L., Campos, N., Caelles, C., Arró, M., and Boronat, A. (1994). *Arabidopsis thaliana* contains two differentially expressed *3-hydroxy-3-methylglutaryl-CoA reductase* genes, which encode microsomal forms of the enzyme. Proc. Natl. Acad. Sci. USA **91:** 927–931.

Flores-Pérez, U., Pérez-Gil, J., Closa, M., Wright, L.P., Botella-Pavía, P., Phillips, M.A., Ferrer, A., Gershenzon, J., and Rodríguez-Concepción, M. (2010). Pleiotropic regulatory locus 1 (PRL1) integrates the regulation of sugar responses with isoprenoid metabolism in *Arabidopsis*. Mol. Plant **3:** 101–112.

Gao, X., Lu, F., Zhou, L., Dang, S., Sun, L., Li, X., Wang, J., and Shi, Y. (2009). Structure and mechanism of an amino acid antiporter. Science **324:** 1565–1568.

Garza, R.M., Tran, P.N., and Hampton, R.Y. (2009). Geranylgeranyl pyrophosphate is a potent regulator of HRD-dependent 3-hydroxy-3-methylglutaryl-CoA reductase degradation in yeast. J. Biol. Chem. **284:** 35368–35380.

Goldstein, J.L., DeBose-Boyd, R.A., and Brown, M.S. (2006). Protein sensors for membrane sterols. Cell **124:** 35–46.

Gonnet, G.H., Cohen, M.A., and Benner, S.A. (1992). Exhaustive matching of the entire protein sequence database. Science **256:** 1443–1445.

Hampton, R.Y. (2002). ER-associated degradation in protein quality control and cellular regulation. Curr. Opin. Cell Biol. **14:** 476–482.

Hampton, R.Y., Gardner, R.G., and Rine, J. (1996). Role of 26S proteasome and *HRD* genes in the degradation of 3-hydroxy-3-methylglutaryl-CoA reductase, an integral endoplasmic reticulum membrane protein. Mol. Biol. Cell **7:** 2029–2044.

Hassink, G., Kikkert, M., van Voorden, S., Lee, S.-J., Spaapen, R., van Laar, T., Coleman, C.S., Bartee, E., Früh, K., Chau, V., and Wiertz, E. (2005). TEB4 is a C4HC3 RING finger-containing ubiquitin ligase of the endoplasmic reticulum. Biochem. J. **388:** 647–655.

Hemmerlin, A., and Bach, T.J. (2000). Farnesol-induced cell death and stimulation of 3-hydroxy-3-methylglutaryl-coenzyme A reductase activity in tobacco cv bright yellow-2 cells. Plant Physiol. **123:** 1257–1268.

Hemmerlin, A., Harwood, J.L., and Bach, T.J. (2012). A raison *d'être* for two distinct pathways in the early steps of plant isoprenoid biosynthesis? Prog. Lipid Res. **51:** 95–148.

Jabs, T., Dietrich, R.A., and Dangl, J.L. (1996). Initiation of runaway cell death in an *Arabidopsis* mutant by extracellular superoxide. Science **273:** 1853–1856.

Jang, J.-C., Fujioka, S., Tasaka, M., Seto, H., Takatsuto, S., Ishii, A., Aida, M., Yoshida, S., and Sheen, J. (2000). A critical role of sterols in embryonic patterning and meristem programming revealed by the *fackel* mutants of *Arabidopsis thaliana*. Genes Dev. **14:** 1485–1497.

Koornneef, M., Alonso-Blanco, C., and Stam, P. (2006). Genetic analysis. Methods Mol. Biol. **323:** 65–77.

Kreft, S.G., and Hochstrasser, M. (2011). An unusual transmembrane helix in the endoplasmic reticulum ubiquitin ligase Doa10 modulates degradation of its cognate E2 enzyme. J. Biol. Chem. **286:** 20163–20174.

Kreft, S.G., Wang, L., and Hochstrasser, M. (2006). Membrane topology of the yeast endoplasmic reticulum-localized ubiquitin ligase Doa10 and comparison with its human ortholog TEB4 (MARCH-VI). J. Biol. Chem. **281:** 4646–4653.

Krogh, A., Larsson, B., von Heijne, G., and Sonnhammer, E.L. (2001). Predicting transmembrane protein topology with a hidden Markov model: Application to complete genomes. J. Mol. Biol. **305:** 567–580.

Learned, R.M. (1996). Light suppresses 3-Hydroxy-3-methylglutaryl coenzyme A reductase gene expression in *Arabidopsis thaliana*. Plant Physiol. **110:** 645–655.

Lee, J.H., Terzaghi, W., Gusmaroli, G., Charron, J.B.F., Yoon, H.J., Chen, H., He, Y.J., Xiong, Y., and Deng, X.W. (2008). Characterization of *Arabidopsis* and rice DWD proteins and their roles as substrate receptors for CUL4-RING E3 ubiquitin ligases. Plant Cell **20:** 152–167.

Leivar, P., Antolín-Llovera, M., Ferrero, S., Closa, M., Arró, M., Ferrer, A., Boronat, A., and Campos, N. (2011). Multilevel control of *Arabidopsis* 3-hydroxy-3-methylglutaryl coenzyme A reductase by protein phosphatase 2A. Plant Cell **23:** 1494–1511.

Leivar, P., González, V.M., Castel, S., Trelease, R.N., López-Iglesias, C., Arró, M., Boronat, A., Campos, N., Ferrer, A., and Fernàndez-Busquets, X. (2005). Subcellular localization of *Arabidopsis* 3-hydroxy-3-methylglutaryl-coenzyme A reductase. Plant Physiol. **137:** 57–69.

Li, H., and Durbin, R. (2009). Fast and accurate short read alignment with Burrows-Wheeler transform. Bioinformatics **25:** 1754–1760.

Li, H., Handsaker, B., Wysoker, A., Fennell, T., Ruan, J., Homer, N., Marth, G., Abecasis, G., and Durbin, R. 1000 Genome Project Data Processing Subgroup (2009). The sequence alignment/map format and SAMtools. Bioinformatics **25:** 2078–2079.

Lovato, M.A., Hart, E.A., Segura, M.J.R., Giner, J.-L., and Matsuda, S.P.T. (2000). Functional cloning of an *Arabidopsis thaliana* cDNA encoding cycloeucalenol cycloisomerase. J. Biol. Chem. **275:** 13394–13397.

Lü, S., Zhao, H., Des Marais, D.L., Parsons, E.P., Wen, X., Xu, X., Bangarusamy, D.K., Wang, G., Rowland, O., Juenger, T., Bressan, R.A., and Jenks, M.A. (2012). *Arabidopsis* ECERIFERUM9 involvement in cuticle formation and maintenance of plant water status. Plant Physiol. **159:** 930–944.

Lumbreras, V., Campos, N., and Boronat, A. (1995). The use of an alternative promoter in the *Arabidopsis thaliana HMG1* gene generates an mRNA that encodes a novel 3-hydroxy-3-methylglutaryl coenzyme A reductase isoform with an extended N-terminal region. Plant J. **8:** 541–549.

Manzano, D., Fernández-Busquets, X., Schaller, H., González, V.C., Boronat, A., Arró, M., and Ferrer, A. (2004). The metabolic imbalance underlying lesion formation in *Arabidopsis thaliana* overexpressing farnesyl diphosphate synthase (isoform 1S) leads to oxidative stress and is triggered by the developmental decline of endogenous HMGR activity. Planta **219:** 982–992.

Masferrer, A., Arró, M., Manzano, D., Schaller, H., Fernández-Busquets, X., Moncaleán, P., Fernández, B., Cunillera, N., Boronat, A., and Ferrer, A. (2002). Overexpression of *Arabidopsis thaliana* farnesyl diphosphate synthase (FPS1S) in transgenic *Arabidopsis* induces a cell death/senescence-like response and reduced cytokinin levels. Plant J. **30:** 123–132.

McGarvey, D.J., and Croteau, R. (1995). Terpenoid metabolism. Plant Cell **7:** 1015–1026.

Meigs, T.E., Roseman, D.S., and Simoni, R.D. (1996). Regulation of 3-hydroxy-3-methylglutaryl-coenzyme A reductase degradation by the nonsterol mevalonate metabolite farnesol in vivo. J. Biol. Chem. **271:** 7916–7922.

Men, S., Boutté, Y., Ikeda, Y., Li, X., Palme, K., Stierhof, Y.-D., Hartmann, M.-A., Moritz, T., and Grebe, M. (2008). Sterol-dependent endocytosis mediates post-cytokinetic acquisition of PIN2 auxin efflux carrier polarity. Nat. Cell Biol. **10:** 237–244.

Newman, J.D., and Chappell, J. (1999). Isoprenoid biosynthesis in plants: Carbon partitioning within the cytoplasmic pathway. Crit. Rev. Biochem. Mol. Biol. **34:** 95–106.

Nicotra, A.B., Atkin, O.K., Bonser, S.P., Davidson, A.M., Finnegan, E.J., Mathesius, U., Poot, P., Purugganan, M.D., Richards, C.L., Valladares, F., and van Kleunen, M. (2010). Plant phenotypic plasticity in a changing climate. Trends Plant Sci. **15:** 684–692.

Nieto, B., Forés, O., Arró, M., and Ferrer, A. (2009). *Arabidopsis* 3-hydroxy-3-methylglutaryl-CoA reductase is regulated at the post-translational level in response to alterations of the sphingolipid and the sterol biosynthetic pathways. Phytochemistry **70:** 53–59.

Orozco-Cardenas, M., and Ryan, C.A. (1999). Hydrogen peroxide is generated systemically in plant leaves by wounding and systemin via the octadecanoid pathway. Proc. Natl. Acad. Sci. USA **96:** 6553–6557.

Phillips, D.R., Rasbery, J.M., Bartel, B., and Matsuda, S.P. (2006). Biosynthetic diversity in plant triterpene cyclization. Curr. Opin. Plant Biol. **9:** 305–314.

Posé, D., Castanedo, I., Borsani, O., Nieto, B., Rosado, A., Taconnat, L., Ferrer, A., Dolan, L., Valpuesta, V., and Botella, M.A. (2009). Identification of the *Arabidopsis dry2/sqe1-5* mutant reveals a central role for sterols in drought tolerance and regulation of reactive oxygen species. Plant J. **59:** 63–76.

Proost, S., Van Bel, M., Sterck, L., Billiau, K., Van Parys, T., Van de Peer, Y., and Vandepoele, K. (2010). PLAZA: A comparative genomics resource to study gene and genome evolution in plants. Plant Cell **21:** 3718–3731.

Rasbery, J.M., Shan, H., LeClair, R.J., Norman, M., Matsuda, S.P.T., and Bartel, B. (2007). *Arabidopsis thaliana* squalene epoxidase 1 is essential for root and seed development. J. Biol. Chem. **282:** 17002–17013.

Rashotte, A.M., Jenks, M.A., Ross, A.S., and Feldmann, K.A. (2004). Novel eceriferum mutants in *Arabidopsis thaliana*. Planta **219:** 5–13.

Räikkönen, J., Mönkkönen, H., Auriola, S., and Mönkkönen, J. (2010). Mevalonate pathway intermediates downregulate zoledronic acid-induced isopentenyl pyrophosphate and ATP analog formation in human breast cancer cells. Biochem. Pharmacol. **79:** 777–783.

Rodríguez-Concepción, M., and Boronat, A. (2002). Elucidation of the methylerythritol phosphate pathway for isoprenoid biosynthesis in bacteria and plastids. A metabolic milestone achieved through genomics. Plant Physiol. **130:** 1079–1089.

Rodríguez-Concepción, M., Forés, O., Martinez-García, J.F., González, V., Phillips, M.A., Ferrer, A., and Boronat, A. (2004). Distinct light-mediated pathways regulate the biosynthesis and exchange of isoprenoid precursors during *Arabidopsis* seedling development. Plant Cell **16:** 144–156.

Schaller, H. (2010). Sterol and steroid biosynthesis and metabolism in plants and microorganisms. Comprehensive Natural Products II Chemistry and Biology **1:** 755–787.

Schnell, J.D., and Hicke, L. (2003). Non-traditional functions of ubiquitin and ubiquitin-binding proteins. J. Biol. Chem. **278:** 35857–35860.

Schrick, K., Fujioka, S., Takatsuto, S., Stierhof, Y.-D., Stransky, H., Yoshida, S., and Jürgens, G. (2004). A link between sterol biosynthesis, the cell wall, and cellulose in *Arabidopsis*. Plant J. **38:** 227–243.

Schrick, K., Mayer, U., Horrichs, A., Kuhnt, C., Bellini, C., Dangl, J., Schmidt, J., and Jürgens, G. (2000). FACKEL is a sterol C-14 reductase required for organized cell division and expansion in *Arabidopsis* embryogenesis. Genes Dev. **14:** 1471–1484.

Schulze, S., Köster, S., Geldmacher, U., Terwisscha van Scheltinga, A. C., and Kühlbrandt, W. (2010). Structural basis of Na(+)-independent and cooperative substrate/product antiport in CaiT. Nature **467:** 233–236.

Smith, M.H., Ploegh, H.L., and Weissman, J.S. (2011). Road to ruin: Targeting proteins for degradation in the endoplasmic reticulum. Science **334:** 1086–1090.

Stone, S.L., Hauksdóttir, H., Troy, A., Herschleb, J., Kraft, E., and Callis, J. (2005). Functional analysis of the RING-type ubiquitin ligase family of *Arabidopsis*. Plant Physiol. **137:** 13–30.

Sugden, C., Donaghy, P.G., Halford, N.G., and Hardie, D.G. (1999). Two SNF1-related protein kinases from spinach leaf phosphorylate and inactivate 3-hydroxy-3-methylglutaryl-coenzyme A reductase, nitrate reductase, and sucrose phosphate synthase in vitro. Plant Physiol. **120:** 257–274.

Suzuki, M., Kamide, Y., Nagata, N., Seki, H., Ohyama, K., Kato, H., Masuda, K., Sato, S., Kato, T., Tabata, S., Yoshida, S., and Muranaka, T. (2004). Loss of function of *3-hydroxy-3-methylglutaryl coenzyme A reductase 1* (*HMG1*) in *Arabidopsis* leads to dwarfing, early senescence and male sterility, and reduced sterol levels. Plant J. **37:** 750–761.

Suzuki, M., Nakagawa, S., Kamide, Y., Kobayashi, K., Ohyama, K., Hashinokuchi, H., Kiuchi, R., Saito, K., Muranaka, T., and Nagata, N. (2009). Complete blockage of the mevalonate pathway results in male gametophyte lethality. J. Exp. Bot. **60:** 2055–2064.

Swanson, R., Locher, M., and Hochstrasser, M. (2001). A conserved ubiquitin ligase of the nuclear envelope/endoplasmic reticulum that functions in both ER-associated and Matα2 repressor degradation. Genes Dev. **15:** 2660–2674.

Theesfeld, C.L., Pourmand, D., Davis, T., Garza, R.M., and Hampton R.Y. (2011). The sterol-sensing domain (SSD) directly mediates signal-regulated endoplasmic reticulum-associated degradation (ERAD) of 3-hydroxy-3-methylglutaryl (HMG)-CoA reductase. J. Biol. Chem. **286:** 26298–26307

Tholl, D., and Lee, S. (2011). Terpene specialized metabolism in *Arabidopsis thaliana*. The *Arabidopsis* Book **9**:e0143. doi:10.1043/tab.0143.

Turnbull, C.G.N., Booker, J.P., and Leyser, H.M. (2002). Micrografting techniques for testing long-distance signalling in *Arabidopsis*. Plant J. **32:** 255–262.

Vembar, S.S., and Brodsky, J.L. (2008). One step at a time: Endoplasmic reticulum-associated degradation. Nat. Rev. Mol. Cell Biol. **9:** 944–957.

Wentzinger, L.F., Bach, T.J., and Hartmann, M.A. (2002). Inhibition of squalene synthase and squalene epoxidase in tobacco cells triggers an up-regulation of 3-hydroxy-3-methylglutaryl coenzyme a reductase. Plant Physiol. **130:** 334–346.

Willemsen, V., Friml, J., Grebe, M., van den Toorn, A., Palme, K., and Scheres, B. (2003). Cell polarity and PIN protein positioning in *Arabidopsis* require STEROL METHYLTRANSFERASE1 function. Plant Cell **15:** 612–625.

Yamashita, A., Singh, S.K., Kawate, T., Jin, Y., and Gouaux, E. (2005). Crystal structure of a bacterial homologue of Na^+/Cl^--dependent neurotransmitter transporters. Nature **437:** 215–223.